1971

The influence of member length on thermal contact resistance in a vacuum environment

Larry Martin Cooper

Department:

THE INFLUENCE OF MEMBER LENGTH ON THERMAL CONTACT RESISTANCE IN A VACUUM ENVIRONMENT

BY

LARRY MARTIN COOPER, 1947-

A THESIS

Presented to the Faculty of the Graduate School of the

UNIVERSITY OF MISSOURI-ROLLA

In Partial Fulfillment of the Requirements for the Degree

MASTER OF SCIENCE IN MECHANICAL ENGINEERING

1971

Approved by

Orlo McNary (Advisor)

E. H. Sauer Jr.

C. Y. Ho

ABSTRACT

An investigation was conducted to determine the influence of member length on thermal contact resistance in a vacuum environment. A model was created which consisted of a center rod axially loaded between two other members. It was assumed that circular macroscopic constriction areas were formed at the contact interface when the rods were loaded. Macroscopic modeling of the contact surfaces makes the thermal contact analysis a function of the mechanical and thermal boundary conditions of the total body.

The method of finite differences was employed to calculate the temperature distribution, heat flows, and thermal contact resistance of each member. Data was created as a function of two parameters: (1) the length of the center rod member and (2) the contact radius.

The results indicate the following. (1) The contact resistance drastically decreases as the center specimen length decreases. This is particularly true if the ratio of member length to member radius, L_1/b, is less than 0.1. (2) At any particular contact radius, the contact resistance at $L_1/b=1$ is twice the contact resistance at $L_1/b=0$. (3) The contact resistance rapidly increases as the contact radius decreases. (4) The interface temperature distribution everywhere in the contact region is non-isothermal. However, the temperature deviations are small and do not exceed five percent.

ACKNOWLEDGEMENT

The author wishes to express his appreciation to Dr. R.O. McNary for suggesting the topics presented in this thesis. The author is grateful for his guidance, encouragement, and advice throughout the investigation.

TABLE OF CONTENTS

LIST OF ILLUSTRATIONS

LIST OF TABLES

NOMENCLATURE

a	radius of contact area
A	apparent contact area
b	radius of rod
d	flatness deviation
E	modulus of elasticity
k	thermal conductivity
L_1	length of lower specimen region
L_2	length of upper specimen region
ΔL	equivalent length of contact resistance
p	contact pressure
q	heat flux
Q	heat flow
r	radial coordinate
R	contact resistance
R_o	radius to center of node
R_t	total resistance
R^*	dimensionless contact resistance
T	temperature
T_i	isothermal temperature of upper region
T_o	isothermal temperature of lower region
ΔT	a temperature difference
x	constriction ratio, $x=a/b$
z	axial coordinate
β	square of grid ratio, $\beta=[\Delta r/\Delta z]^2$
δ	grid spacing, $\delta=\Delta r=\Delta z$

γ ratio, $\gamma=\Delta r/2R_o$

ϕ dimensionless interface temperature deviation

ζ elastic conformity modulus

ω relaxation parameter

INTRODUCTION

A considerable effort has been expended in the area of thermal contact resistance. Investigations have attempted to correlate contact resistance to contact pressure, surface roughness, material properties and other parameters. Some investigations deal with either the experimental measurement or theoretical prediction of thermal contact resistance for models with contact regions filled with interstitial fluids. Such efforts have been fruitful in the development of high conducting fluids for rapid heat transfer within contact regions (e.g. silicone compounds).

Associated with some of these investigations are theoretical models which base the contact resistance phenomena upon a microscopic viewpoint. The subsequent results, as derived from such an approach, have been reliable for contact regions coated with oil, silicone grease, sodium, and others. However, such microscopic models are inadequate for contact regions located in vacuum environments where no interfacial fluids are present.

The macroscopic modeling approach has overcome some of the deficiencies of microscopic modeling. With the macroscopic approach thermal contact resistance becomes a function, <u>not</u> only of the complex physics and chemistry of a contact interface as associated with the microscopic approach, but <u>also</u> of the mechanical and thermal boundary conditions of the <u>total</u> body. Recent success has been attained in predicting thermal contact resistance for single contact models located in a vacuum environment. Such models, developed from

a macroscopic viewpoint, have greatly contributed to the understanding of contact resistance.

The objective of this investigation is to extend the macroscopic approach to a study of the influence of member length upon thermal contact resistance. Such an influence has not been considered by other investigators, as their efforts have mainly concentrated on the influence of the contact surface.

REVIEW OF LITERATURE

The following is a collection of the major investigations devoted to the study of thermal contact resistance in a vacuum.

Jacobs and Starr [1], in one of the first published reports, investigated the problem of thermal contact resistance associated with the use of mechanical thermal switches in cryogenic apparatus. The study attempted to relate the effect of pressure on interface conductance. Gold, silver, and copper - all excellent conductors - with "optically flat" surfaces were used with contact pressures ranging from approximately zero to 2.5 kg/cm^2. Data was presented for (1) room temperature and (2) the temperature of boiling nitrogen ($-195^{\circ}C$). The conductances were found to be several times greater at room temperature than at the liquid nitrogen temperature. The report did not give the vacuum pressure, quantitative flatness deviation, nor the specimen's hardness.

Berman [2] also worked with the problem of thermal switches for low temperature work, examining their potential as mechanical heat switches. Of main interests in the study were (1) dependence of conductance with load, (2) variation of conductance with temperature, and (3) applicability of the Wiedmann-Franz-Lorenz relation. The experiments were conducted with steel and copper specimens in a vacuum of 10^{-4} torr over temperatures ranging from 1.8 to $77^{\circ}K$. It was found that the conductances were proportional to T^2 at helium temperatures ($4.2^{\circ}K$), but were of small dependence at nitrogen temperatures. The electrical conductances obtained from the Wiedmann-Franz-

Lorenz law were always much less than the thermal conductances. The conductances of the copper and steel varied differently during load cycles. This suggested that significant heat transfer occurred through electircal insulating regions of the specimen surfaces.

Another experimental study was performed by Mikesell and Scott [3]. They investigated heat conduction through insulating supports of storage vessels for cryogenic liquids. Two types of supports, (1) multiple-contacts in the form of stacks of thin metallic plates and (2) non-metallic spheres, were tested in a 10^{-5} torr pressure environment with boundary temperatures of either 76 and 296^{o}K or 20 and 76^{o}K. The results showed that the heat conduction for a stack of 0.008 inch thick stainless steel plates under a 1000 psi load was only two percent of the heat conduction of a solid sample of identical dimensions exposed to the same load and temperatures. The results furthermore showed that the contact resistance remained high for multiple contacts under large apparent contact pressures.

Fried and Costello [4] published a study concerned with the thermal contact resistance of plates within a space environment, i.e., ambient pressures from 10^{-4} to 10^{-6} torr. The plates, 5x5x1/8 inches, were subjected to contact pressures from a few psi to 35 psi. The specimens used were aluminum and magnesium having surface finishes between six and 65 rms. Graphical data showed the variation of interface conductance with contact pressure. The parameters associated with these plots included surface finish, flatness deviation, specimen material, and shim material (if present). Fried and

Costello's results indicated that (1) flatness deviation and surface roughness immensely effected the contact resistance, (2) soft shim materials appreciably improved interface conductance, and (3) thermal contact resistance is highly pressure dependent at low contact pressures. It was found that at higher pressures the conductance verses pressure curve becomes less steep. The difference in modulus of elasticity of the specimens and soft shim material had a significant influence on the conductance.

Clausing and Chao [5] and Clausing [6] investigated the thermal contact resistance across two cylindrical rods in axial contact in a vacuum environment. Theoretical analysis of thermal contact resistance prior to that of Clausing and Chao's, such as those of Cetinkale and Fishenden [7], L.C. Laming [8], and Fenech and Rohsenow [9], had defined the contact area from a microscopic viewpoint, i.e., a summation of microscopic constrictions. The difficulty of such an approach is in the prediction of number, size, and location of these microscopic contact areas. Investigators have tried to relate the number, size, and location of microscopic contacts to such properties as surface finish and material hardness. However, such relationships have failed to explain the total physics and chemistry of contact surfaces. Clausing and Chao lumped the microscopic contacts into one macroscopic area. They defined a macroscopic area as an area containing a high density of microscopic contacts.

Clausing and Chao proposed that conduction through the macroscopic constriction area was the dominant mode of heat transfer across their axial contact model. They further proposed that in a vacuum

environment with highly polished specimens, interstitial conduction and radiation heat transfer are negligible contributors. A theoretical model was developed to predict the thermal contact resistance as influenced by such parameters as contact area, material properties, and thermal strain. An extensive experimental investigation was undertaken to confirm the predicted influence of these parameters upon the contact resistance. The experimental results correlated with the predicted results. From their results, Clausing and Chao concluded that (1) macroscopic constriction dominated the thermal contact resistance for a majority of engineering surfaces and (2) the macroscopic model made prediction of thermal contact resistance across a contact possible when macroscopic constriction dominated. A transient method of analysis, as proposed by M.P. Laurent and H.J. Sauer, Jr. [10], has verified the trends predicted by Clausing [6].

The theoretical model solved by Clausing and Chao had a mixed boundary condition, that of (1) an isothermal temperature condition within the contact region and (2) zero heat flux in the remaining annular non-contact region. Clausing employed a finite difference solution of the model to account for this mixed boundary condition. Roess [11], in an analytic solution, circumvented the mixed boundary conditions with an expression for the heat flux distribution across the contact area. For a contact radius, a, Roess found that a flux distribution which was proportional to

$$[1-r^2/a^2]^{-1/2} \quad , \quad 0 < r < a \qquad \text{----------} \qquad 1$$

resulted in an approximately isothermal contact area unless the

constriction ratio, x=a/b, (b is the radius of the rod) was near unity. At unity the constriction area equals the apparent contact area. Roess made an additional assumption - that the ratio of rod length to radius, L/b, was sufficiently large so as to not affect the thermal contact resistance. The assumptions of Roess' flux distribution restrict its applicability. The results of Clausing show that significant changes in the thermal contact resistance across a single contact occur when L/b is small.

It should be noted, however, that the model proposed by Clausing and Chao employs isothermal boundary conditions which are physically unrealistic for small L/b ratios. The construction of the model makes an examination of the influence of member length on thermal contact resistance not possible.

From a survey of literature, the most promising results in the area of thermal contact resistance in a vacuum have been from the works of Clausing and Chao. However, to the knowledge of this investigator, the influence of member length on thermal contact resistance has not been examined.

FORMULATION OF THE MODEL

When heat flows through two members in contact, an additional temperature drop ΔT occurs. This additional drop is due to the constricted area of contact between the two members. This constricted area produces a resistance to heat flow which is commonly known as thermal contact resistance.

In the traditional definition, the contact resistance, R, is given by the equation:

$$R = \Delta T/[Aq] \qquad (2)$$

where A is the apparent contact area, q is the heat flux, and ΔT is the temperature difference between the two member surfaces in contact.

Heat can be transferred across the contact by three different modes. They are (1) thermal radiation, (2) interstitial conduction, and (3) metal-to-metal contact. Investigations [5,6] have shown that in a vacuum environment thermal radiation and interstitial conduction are negligible in comparison with metal-to-metal conduction for clean engineering surfaces subjected to engineering loads. Modeling of a single contact region, based upon macroscopic metal-to-metal constriction, has been successful in predicting the contact resistance across this single contact [5].

It was sought to produce a model which is capable of predicting the influence that the member length has upon the constriction resistance. Figure 1 represents the model that was investigated.

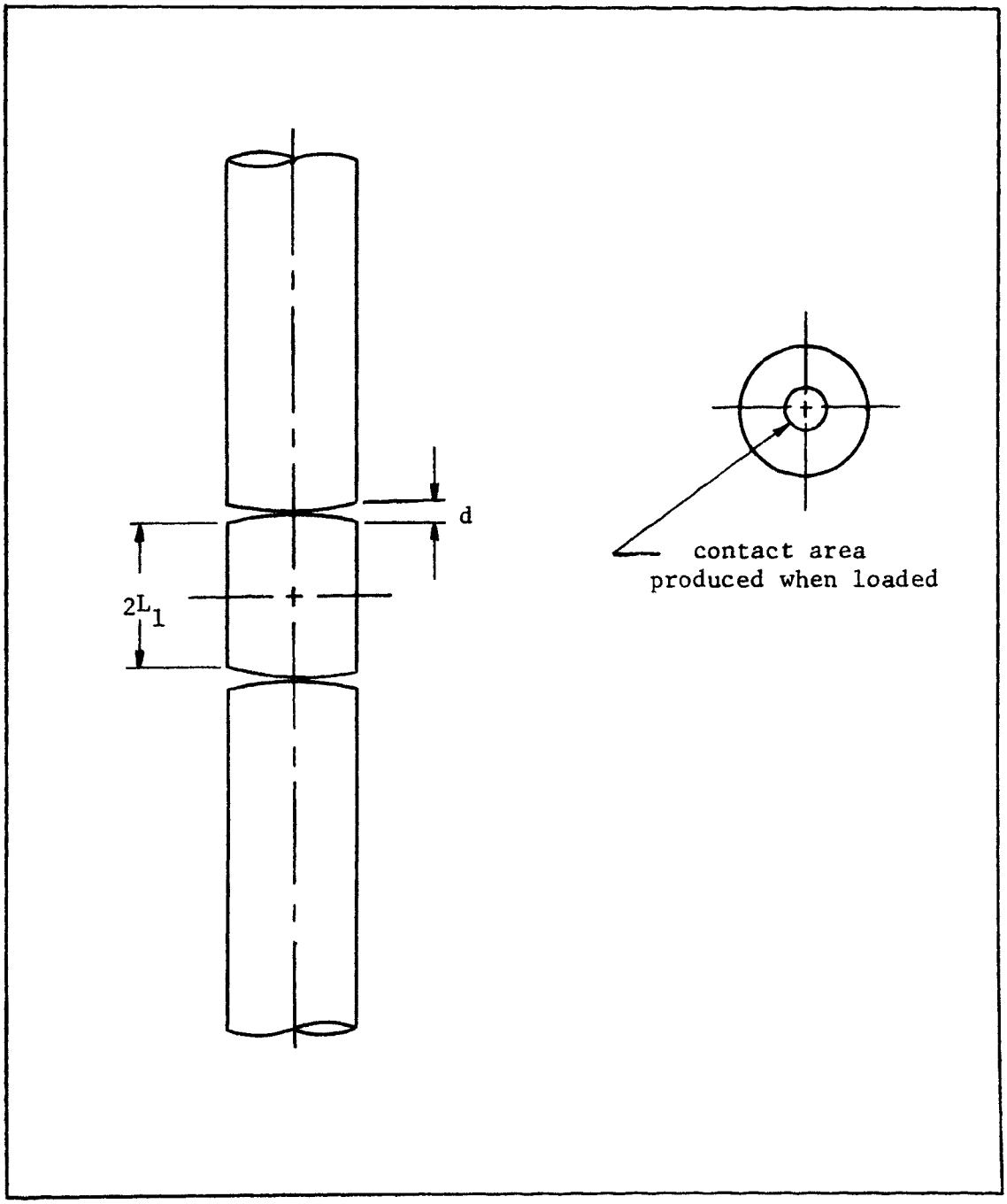

Figure 1. Proposed Model

The model consists of a center rod which is axially loaded between two other rods. Two axial contacts exist between the three rods. The surfaces in contact are assumed to be spherical caps of small flatness deviation (in the range of 10 to 200 μinches) which produce circular contact areas when loaded. All flatness deviations are assumed to be identical. The surfaces are furthermore considered to be highly polished and free of any oil, dirt, or oxide films. It is assumed that no interfacial fluids are present. The ends of each outer rod are subjected to different isothermal temperatures. The lengths of the outer rods are equal and are of sufficient length to be far removed from the contact region. The length of the center cylinder will be varied. The thermal conductivity and modulus of elasticity are also assumed to be identical for all three rods.

The symmetry of the geometry simplifys the mathematical solution. Figure 2 represents the mathematical geometry to be solved. Because of symmetry, an isothermal temperature occurs radially at half the axial length of the center rod. The following partial differential equation and boundary conditions apply:

$$\frac{\partial^2 T}{\partial r^2} + [1/r]\frac{\partial T}{\partial r} + \frac{\partial^2 T}{\partial z^2} = 0 \qquad (3)$$

$$T(r,0) = T_o \qquad (4)$$

$$\frac{\partial T}{\partial r}(b,z) = 0 \quad , \quad 0 < z < (L_1+L_2) \qquad (5)$$

$$\frac{\partial T}{\partial z}(r,L_1) = 0 \quad , \quad a < r < b \quad \text{(both regions)} \qquad (6)$$

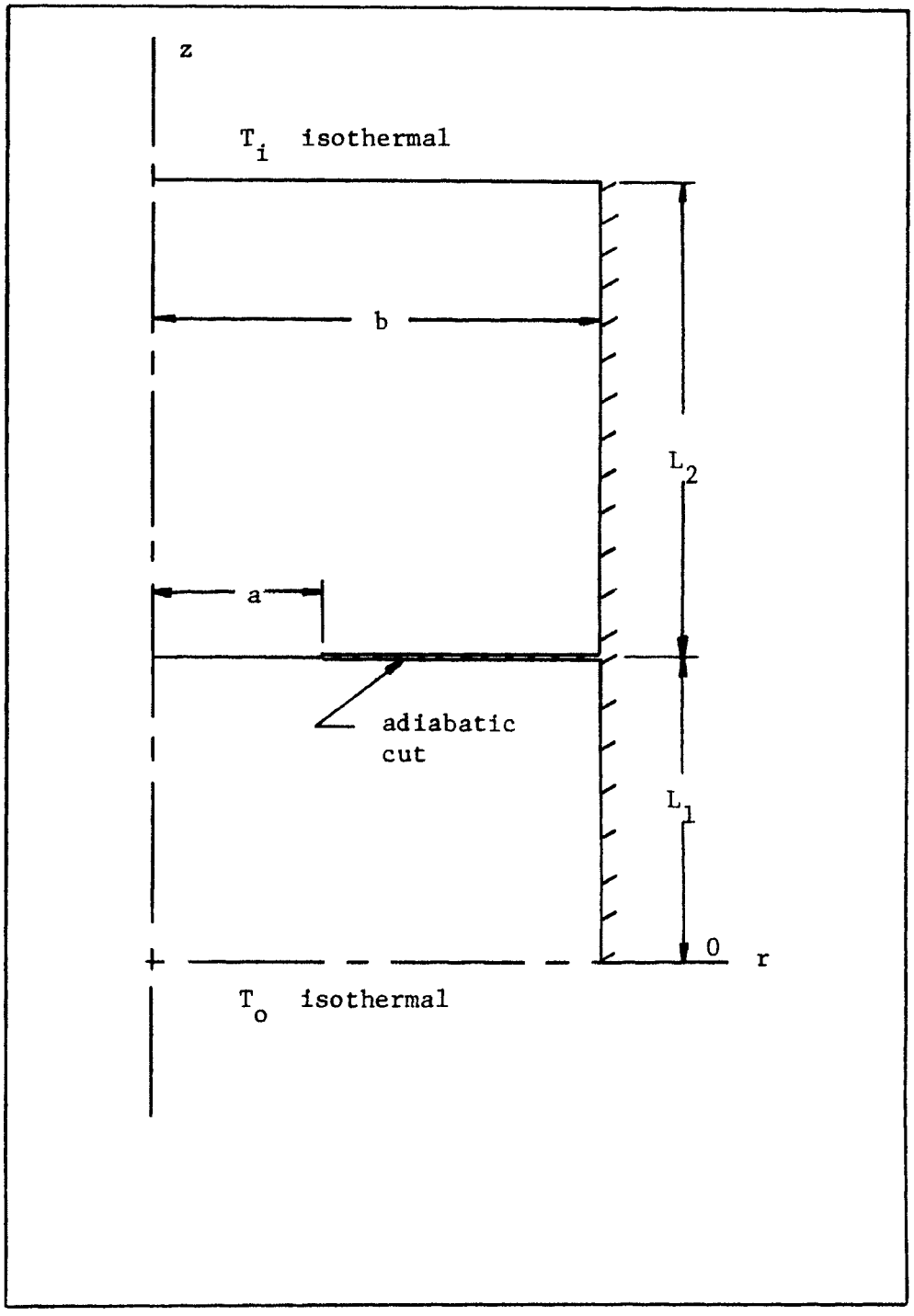

Figure 2. Simplified Mathematical Model

$$T(r,L_1+L_2) = T_i \quad \text{----------} \quad (7)$$

The adiabatic cut in Figure 2 represents an annular region of no contact between the two members. The boundary conditions which apply along the curved surface at the non-contact region may be applied along the line $z=L_1$, because the flatness deviation is several orders of magnitude smaller than the other dimensions of the body.

METHOD OF SOLUTION

In order to calculate thermal contact resistance, it is required that the heat flow passing through the rods be known. Therefore, the temperature field within the region must first be determined.

Since the geometry and mixed boundary conditions of the problem make its solution very formidable, it was elected to employ the method of finite differences to solve the problem.

The model was divided into a network of nodes. The mass and associated temperature distribution within the model are distributed among the interconnecting mesh of nodes. The temperature at any node is determined by performing an energy balance on that node. An energy balance on each node produces a characteristic temperature equation amenable for an iteration scheme. The temperature equations used for iteration are cataloged in Appendix A.

With all the nodes within the region classified with their appropriate temperature equation, an iterative scheme was employed to obtain the correct node temperatures. The temperatures, as well as all other data, were solved using an IBM 360-50 computer at the University of Missouri-Rolla, Rolla, Missouri. Because the number of nodes at times approached 3000, additional programming techniques were employed to minimize the time required for computation.

Since the execution time required for an iterative process is highly dependent upon the number of nodes, a coarse network of nodes was initially created and their respective temperatures calculated.

A nodal spacing one-third finer was then created. The reduction of the node spacing by one third kept a particular contact radius fixed at its location regardless of the node spacing. The initial temperatures for the fine network were obtained from an extrapolation of the final temperatures obtained in the coarse network solution. The indicator that the solution for a particular set of equations had converged was a check of the heat balance. The iteration procedure was stopped when the difference in the heat passing through the top of the upper region and the heat passing through the bottom of the lower region was less than 0.5 percent.

Convergence was further accelerated using the extrapolated Liebmann method [12]. This method accelerated the rate of convergence over that of the Gauss-Seidel iteration scheme. An optimal relaxation factor, ω=1.7, was obtained from trial and error runs. The final iterative scheme which was developed proved to be an efficient and stable method.

RESULTS AND DISCUSSION

It was sought to determine the influence that (1) variance of the center member length and (2) variance of the constriction radius has upon the thermal contact resistance. The contact resistance is determined as follows. The total resistance, R_t, is determined by:

$$R_t = |T_i - T_o|/Q \quad \text{----------} \quad 8$$

T_i is the isothermal temperature of the upper region and T_o is the isothermal temperature of the lower region. Q is the average of the heat flow across the upper top region and the heat flow across the lower bottom region. (The differences in the two values never exceeded 0.5 percent in any of the results.) The constriction resistance, R, is then computed by subtracting the internal resistance of the rods from the total resistance, or:

$$R = R_t - [L_1 + L_2]/[k\pi b^2] \quad \text{----------} \quad 9$$

For convenience non-dimensional terms are created by dividing the member length, L_1, and the contact radius, a, by the radius of the cylinder. This yields L_1/b and $x=a/b$, respectively. A non-dimensional contact resistance, R^*, is created as follows:

$$R^* = k\pi Rb = \Delta L/b \quad \text{----------} \quad 10$$

The term ΔL may be interpreted as the additional length of rod required to produce the constriction.

An extrapolation procedure was used to correct for spatial truncation errors. For any node size used in a solution, an error exists in the value of the contact resistance. This error is associated with the mesh size, δ, or node spacing of the network. It was found that his error is a linear function of δ. Graphical analysis of R^* verses node spacing revealed the linearity. Since values of R^* for a particular solution were calculated for a series of mesh sizes, the value of the constriction resistance, R^*, was obtained by extrapolating to $\delta=0$. Figure 3 illustrates the concept employed. A tabulation of data for the non-dimensional constriction resistance, R^*, is given in Appendix B.

A benefit of the extrapolation procedure is a method of bounding the error in the results. Upper and lower bound values of R^* were computed using the heat flow at the top of the upper region, $Q=Q_{z=L_1+L_2}$, and the heat flow at the bottom of the lower region, $Q=Q_{z=0}$, respectively. These values of heat flow were used on the assumption that the actual heat flow lies between the value of heat flow in and heat flow out of the regions. As shown in Figure 3, the bounded values were projected onto $\delta=0$. Bounded percent deviations, as tabulated in Appendix B, were calculated for each constriction resistance.

The correctness of this extrapolation method, as well as the validity of the programming, was confirmed with the correlation of data sets $L_1/b=0$ and $L_1/b=1$ with that of Clausing [6]. When $L_1/b=0$, the model reduces to that of Clausing's. When $L_1/b=1$, the results

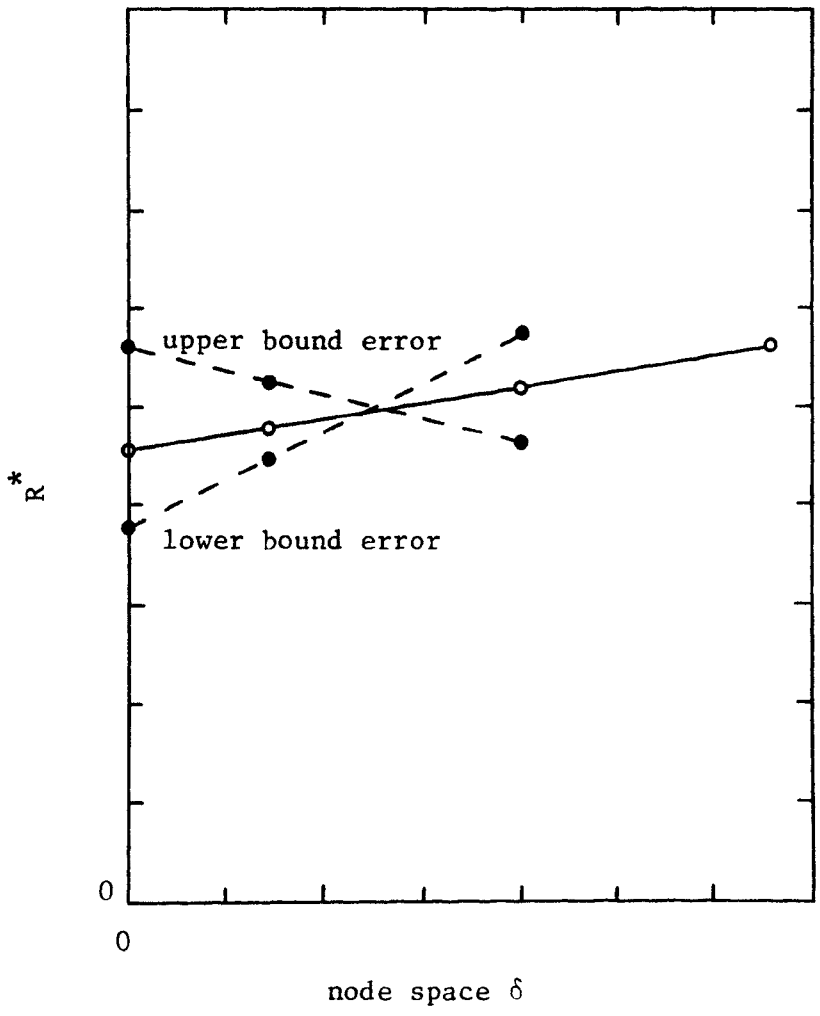

Figure 3. Typical Extrapolation Analysis

for R^* are twice the value for $L_1/b=0$.

Figure 4 describes the influence that the member length, L_1/b, has upon the non-dimensional constriction resistance, R^*, for a family of constriction radii, x. As expected, the respective constriction resistances increased as the contact radii decrease. Of significance are the large changes in the constriction resistance for small L_1/b values. The changes become more dramatic as the constriction radius decreases. As an aid in analysis, a one dimensional model (see Appendix C) was developed for prediction of the constriction resistance, R^*, at small L_1/b values. The resulting equation developed from the model is:

$$R^* = R^*_{L_1=0} + [L_1/b][1/x^2-1] \quad \text{----------} \quad 11$$

As can be seen, the predicted curves approach the curves generated from equation (11) as L_1/b approaches zero. The implication of these curves suggests that as the member length, L_1/b, approaches zero, one-dimensional heat transfer in the axial direction becomes the dominant path.

Figure 5 shows the influence that the constriction radius, x, has upon the non-dimensional contact resistance, R^*. As can be seen, the contact resistance rapidly increases as the contact radius decreases. The graph also reveals that the member length, L_1/b, must be small before a significant shift in the curves occur.

At present, it is experimentally difficult to accurately measure the circular radius of a contact area produced when such an

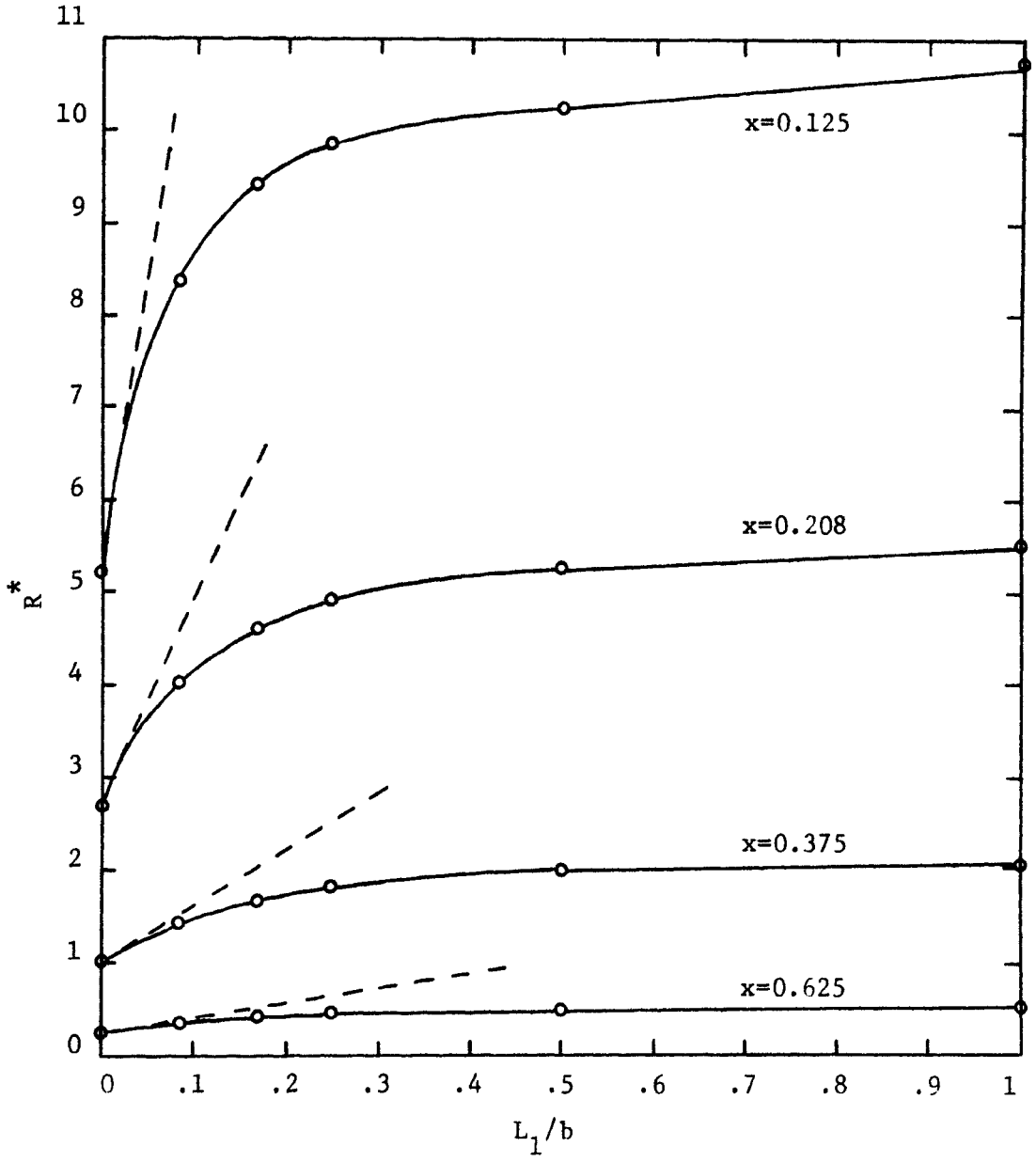

Figure 4. Influence of Member Length on Dimensionless Constriction Resistance

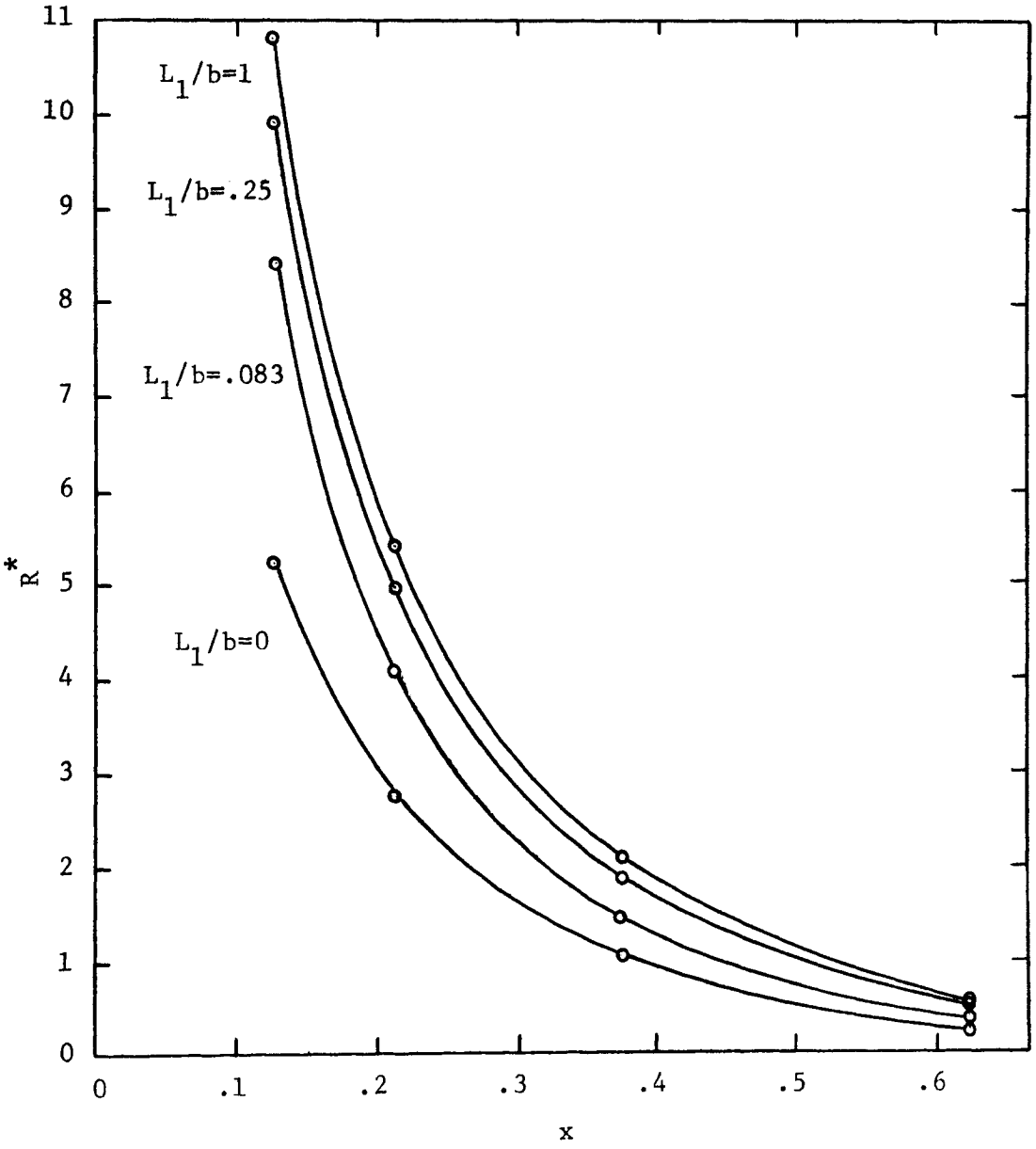

Figure 5. Influence of Constriction Radius on Dimensionless Constriction Resistance

interface is loaded. However, the assumed spherical surface profiles allow the application of the Hertz [13] contact stress formulation to relate loading of the cylinders to the constriction radius, x. Clausing and Chao [5] have shown that if the lengths of the members in contact are large in comparison to the contact radius, a, and if the modulus of elasticity and Poisson's ratio of all members are identical, then the elastic conformity modulus, ζ, is related to the contact radius as follows:

$$\zeta = [x/1.285]^3 \quad , \quad 0 < x < 0.65 \qquad (12)$$

where:

$$\zeta = [pb][Ed] \qquad (13)$$

The symbol p denotes the apparent contact pressure on the rods, E is the modulus of elasticity of the material, d is the combined flatness deviation of the contact surfaces and b is the radius of the rod. A Poisson's ratio of 0.315 was employed to obtain equation (12).

Figure 6 relates the influence of the elastic conformity modulus to R^*. The graph should provide an aid to an experimental investigation of the model by R. Shockley, under the supervision of Dr. R.O. McNary at the University of Missouri-Rolla, Rolla, Missouri.

It was found that Clausing's numerical results, when reconstructed, agreed closely with the data herein (see Appendix D). Since Clausing's model always requires the existence of an isothermal temperature at the contact interface, an examination of the inter-

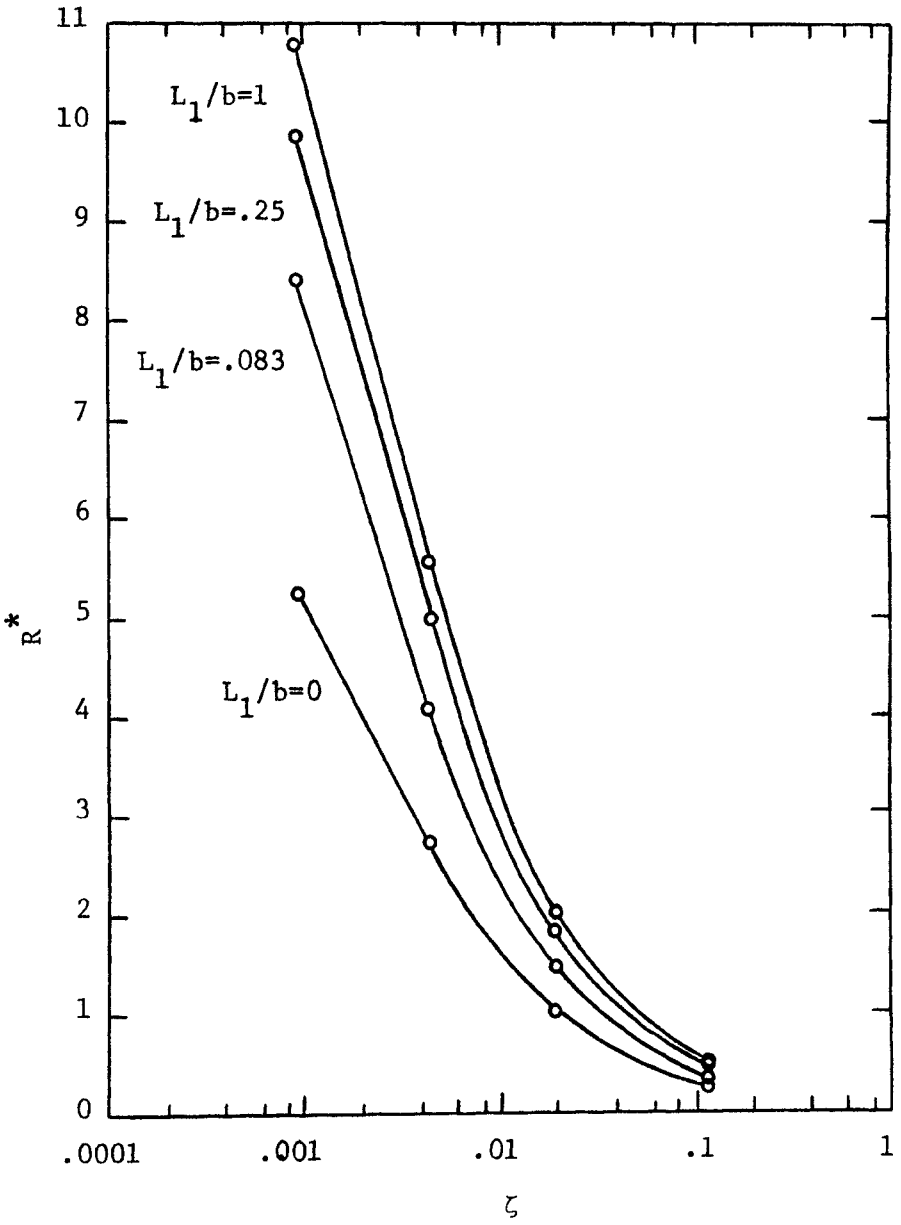

Figure 6. Influence of Elastic Conformity Modulus on Dimensionless Constriction Resistance

face temperatures was conducted for the center member length model. Figure 7 represents the results which were obtained. The graph plots dimensionless interface temperature deviation as a function of member length, L_1/b. Dimensionless interface temperature deviation was defined as:

$$\phi = [\Delta T_{\text{max at interface}}]/[T_i - T_0][100\%] \quad \text{----------} \quad 14$$

The deviation is zero at $L_1/b=0$, as expected. A maximum deviation, whose value is uncertain, occurs between $0.1 < L_1/b < 0.2$. At $L_1/b=1$ the deviation is again zero. The relative deviations indicate that for $0 < L_1/b < 1$ the interface temperature distribution is non-isothermal. However, the deviations are less than five percent. Such small deviations suggest that the non-isothermal temperature differences across an interface are too small to appreciably alter the results from that of the solution associated with an isothermal interface boundary condition.

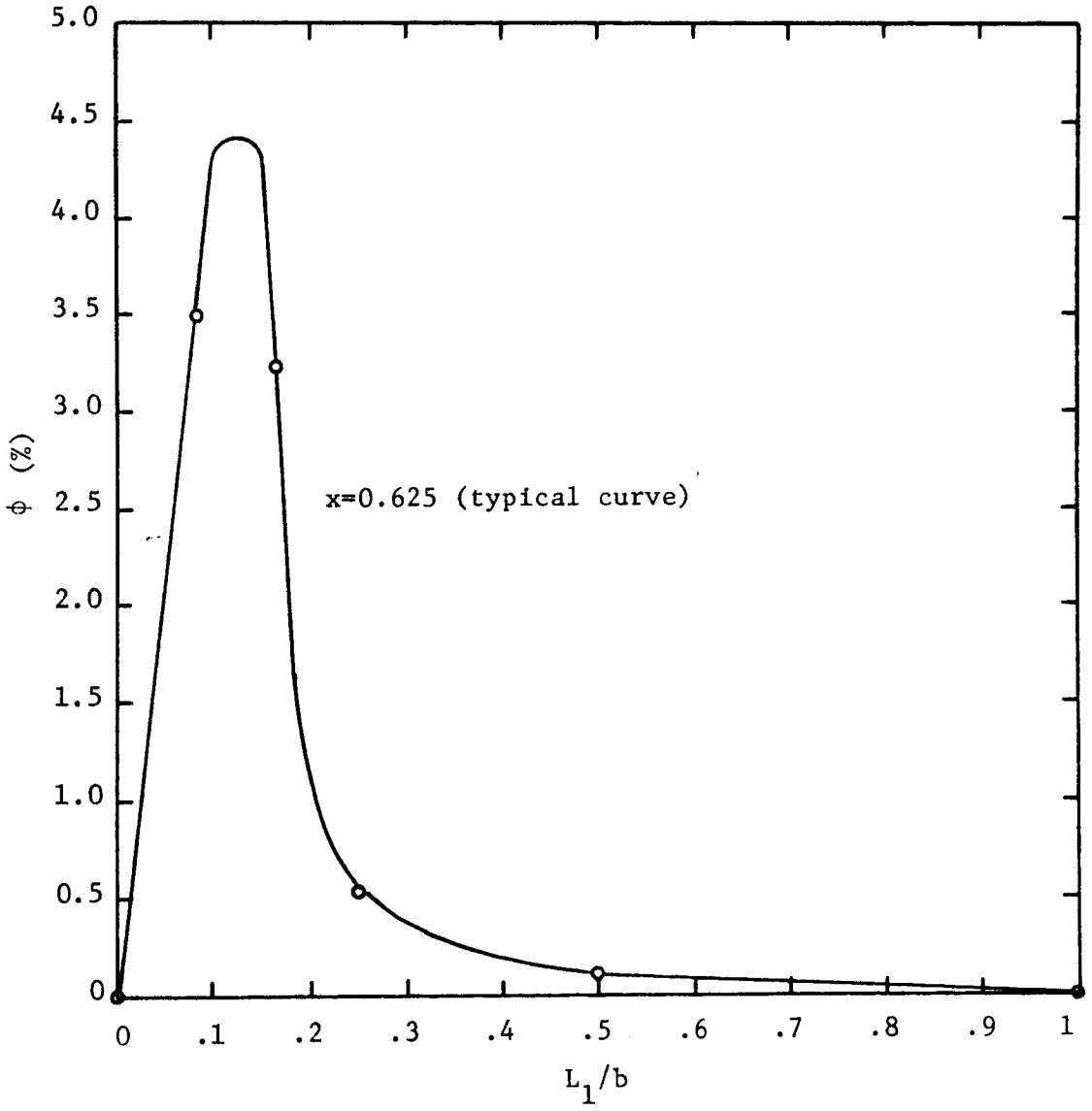

Figure 7. Dimensionless Interface Temperature Deviation verses Member Length

CONCLUSIONS

The investigation conducted produced a model, composed of a center member axially loaded between two outer rods, which predicts the influence of the center specimen length, contact radius, and elastic conformity modulus on thermal contact resistance in a vacuum environment. The model was constructed assuming macroscopic constriction as the path of heat transfer across the contacts. Such an assumption makes the thermal contact analysis of the model a function of the mechanical and thermal boundary conditions of the total body. The constrictions areas were assumed to be circular when the rods were loaded.

Four major findings can be concluded from the results. They are:

1. The contact resistance drastically decreases as the center specimen length decreases. This is particularly true if the ratio of the length of the center member to the radius of the cylinder, L_1/b, is less than 0.1.

2. The value of contact resistance, R^*, at $L_1/b=1$ is twice that of $L_1/b=0$ at any particular contact radius.

3. The effect of member length is of greater significance for smaller contact radii.

4. The interface temperature distribution of a contact area is non-isothermal. However, the deviation of the temperature from an isothermal condition is relatively small, never exceeding five percent.

Successful correlation between predicted and experimental results have been achieved for single contact models using two cylinders. Such a precedence is a hopeful indication of the success of the model herein. An experimental investigation underway will test the validity of the predictions presented.

In conclusion, the investigation positively indicates that member length has a significant influence upon thermal contact resistance in a vacuum environment.

BIBLIOGRAPHY

1. R.B. Jacobs and C. Starr, "Thermal Conductance of Metallic Contacts," Rev of Scientific Instruments, Vol. 10, 1939, pp. 140-141.

2. R. Berman, "Some Experiments of Thermal Contact at Low Temperatures," Journal of Applied Physics, Vol. 27, No. 4, April, 1956, pp. 318-323.

3. R.P. Mikesell and R.B. Scott, "Heat Conduction Through Insulating Supports in Very Low Temperature Equipment," Journal of Research of the National Bureau of Standards, Vol. 57, 1956, pp. 371-376.

4. E. Fried and F.A. Costello, "Interface Thermal Contact Resistance Problems in Space Vehicles," American Rocket Society Journal, Vol. 32, 1962, pp. 237-243.

5. A.M. Clausing and B.T. Chao, "Thermal Contact Resistance in a Vacuum Environment," A.S.M.E. Transactions-Series C, Vol. 87, May, 1965, pp. 243-251.

6. A.M. Clausing, "Some Influences of Macroscopic Constrictions on the Thermal Contact Resistance," Univ. of Illinois Eng. Exp. Station Report ME-TN-242-2, 1965.

7. T.M. Cetinkale and M. Fishenden, "Thermal Conductance of Metal Surfaces in Contact," International Conference on Heat Transfer, The Institution of Mechanical Engineers, London, 1951.

8. L.C. Laming, "Thermal Conductance of Machined Metal Contacts," 1961 International Heat Transfer Conference, Part 1, No. 8, Boulder, Colorado, September, 1961, pp. 65-76.

9. H. Fenech and W.M. Rohsenow, "Predicition of Thermal Conductance of Metallic Surfaces in Contact," A.S.M.E. Transactions-Series C, Vol. 85, February, 1963, pp. 15-22.

10. M.P. Laurent and H.J. Sauer, Jr., "Transient Analysis of Thermal Contact Resistance," AIAA 6th Thermophysics Conference, Tullahoma, Tenn., AIAA Paper No. 71-438, April 26-28, 1971.

11. L.C. Roess, "Theory of Spreading Conductance," Appendix A of an Unpublished Report of the Beacon Laboratories of Texas Company, Beacon, New York.

12. G.D. Smith, Numerical Solutions of Partial Differential Equations, Oxford University Press, New York, p. 29.

13. S. Timoshenko and J.N. Goodier, Theory of Elasticity, McGraw-Hill Book Co., New York, 1951, p. 375.

VITA

Larry Martin Cooper was born on November 3, 1947, in St. Louis, Missouri.

He entered the University of Missouri-Rolla in Rolla, Missouri, in September 1965 and graduated in June 1969 with a Bachelor of Science degree in Mechanical Engineering.

He has been enrolled in the Graduate School of the University of Missouri-Rolla in Rolla, Missouri, since June 1969.

APPENDICES

APPENDIX A - Temperature Equations

The eight different node types present in the mathematical model, which are referred to in Figure 8, are used in the method of finite difference. Note: $\beta=\Delta r^2/\Delta z^2=1$ and $\gamma=\Delta r/2R_o$

1. $T_{i,j} = [[1+\gamma]T_{i+1,j}+[1-\gamma]T_{i-1,j}+\beta[T_{i,j+1}+T_{i,j-1}]]/[2+2\beta]$

2. $T_{i,j} = [4T_{i+1,j}+\beta[T_{i,j+1}+T_{i,j-1}]]/[4+2\beta]$

3. $T_{i,j} = [2[1-\gamma]T_{i-1,j}+\beta[1-\gamma/2][T_{i,j+1}+T_{i,j-1}]]/[2+2\beta-2\gamma-\beta\gamma]$

4. $T_{i,j} = [[1+\gamma][T^u_{i+1,j}+T^l_{i+1,j}]+2[1-\gamma]T_{i-1,j}+2\beta[T_{i,j+1}+T_{i,j-1}]]/[4+4\beta]$

5. $T_{i,j} = [[1+\gamma]T_{i+1,j}+[1-\gamma]T_{i-1,j}+2\beta T_{i,j+1}]/[2\beta+2]$

6. $T_{i,j} = [[1+\gamma]T_{i+1,j}+[1-\gamma]T_{i-1,j}+2\beta T_{i,j-1}]/[2\beta+2]$

7. $T_{i,j} = [[1-\gamma]T_{i-1,j}+\beta[1-\gamma/2]T_{i,j+1}]/[1+\beta-\gamma-\beta\gamma/2]$

8. $T_{i,j} = [[1-\gamma]T_{i-1,j}+ [1-\gamma/2]T_{i,j-1}]/[1+\beta-\gamma-\beta\gamma/2]$

$T^u_{l+1,j}$ and $T^l_{i+1,j}$ in temperature equation (4) refer to upper region node temperature and lower region node temperature, respectively.

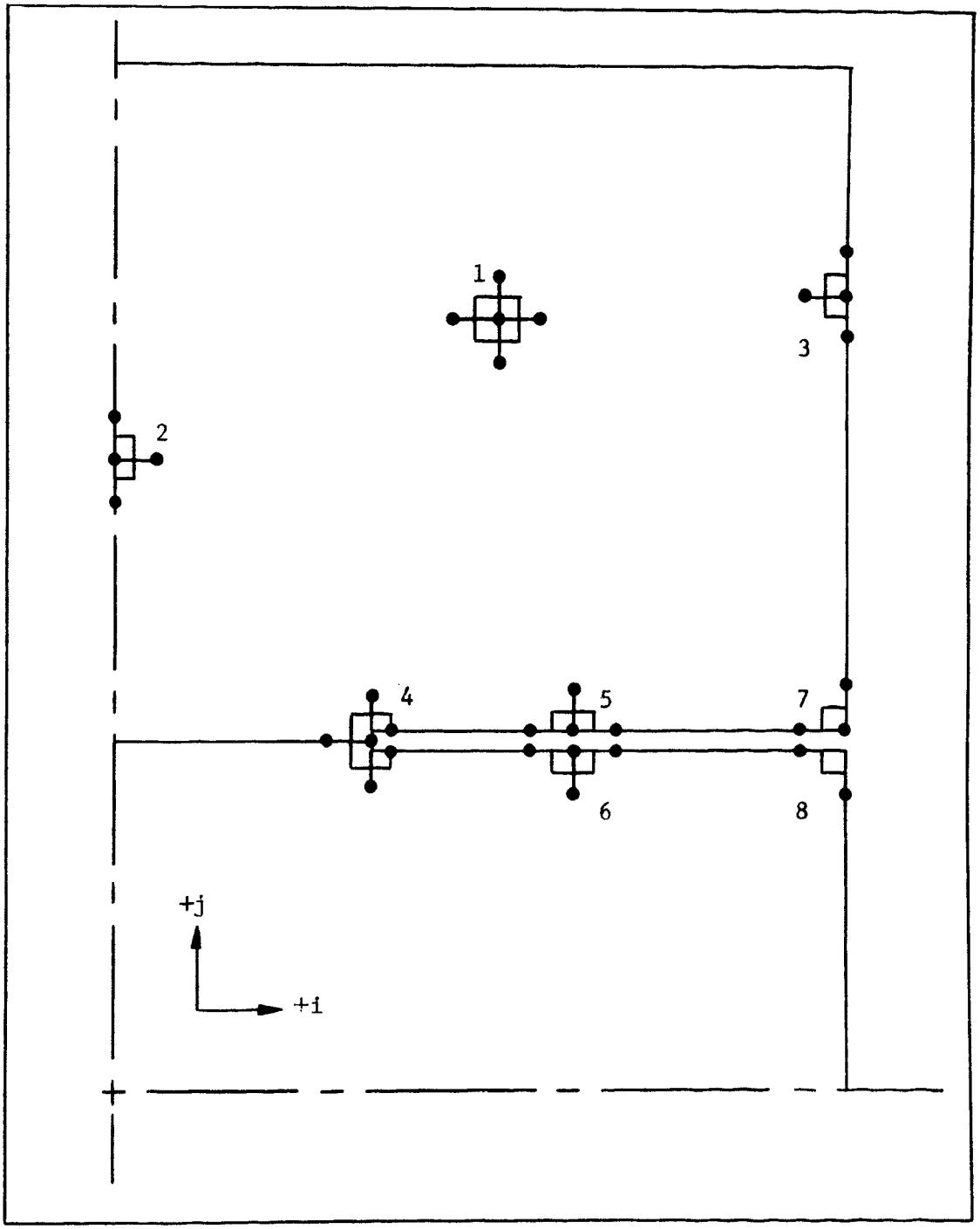

Figure 8. Temperature Nodes

APPENDIX B - Tabulation of Results

x	L_1/b	R^*	+ dev %	- dev %
0.875	0	0.0243	7.40	7.42
0.875	0.083	0.0434	0.35	0.35
0.875	0.167	0.0473	1.34	1.34
0.875	0.250	0.0482	1.97	1.97
0.875	0.500	0.0482	3.16	4.40
0.875	1.000	0.0490	1.31	1.31
0.625	0	0.2607	1.05	1.05
0.625	0.083	0.3795	0.45	0.45
0.625	0.167	0.4411	0.52	0.52
0.625	0.250	0.4775	0.90	0.91
0.625	0.500	0.5132	1.34	1.35
0.625	1.000	0.5271	0.42	0.42
0.375	0	1.0298	1.02	1.03
0.375	0.083	1.4607	0.64	0.64
0.375	0.167	1.6994	0.52	0.52
0.375	0.250	1.8491	0.55	0.55
0.375	0.500	2.0147	0.89	0.89
0.375	1.000	2.0739	0.22	0.21
0.208	0	2.7126	1.62	1.64
0.208	0.083	4.0382	0.72	0.72
0.208	0.167	4.6514	0.50	0.50
0.208	0.250	4.9758	0.59	0.59
0.208	0.500	5.2986	1.27	1.28
0.208	1.000	5.5378	0.56	0.56
0.125	0	5.2446	0.81	0.82
0.125	0.083	8.4121	0.24	0.24
0.125	0.167	9.4678	0.48	0.49
0.125	0.250	9.9051	0.62	0.61
0.125	0.500	10.283	1.33	1.35
0.125	1.000	10.827	0.60	0.61

Table I. Tabulated Results

APPENDIX C - Development of a One-Dimensional Model

It is assumed that one-dimensional heat conduction is dominant in the lower specimen for small values of L_1 (see Figure 9). T_1, T_2, and T_3 are considered to be isothermal temperatures. T_2 is an isothermal temperature at the interface. The following equations are derived from the model.

$$Q = [T_3-T_1]/[R_1+R_2]$$

$$R^* = [[T_3-T_1]/Q-[L_1+L_2]/[k\pi b^2]][k\pi b]$$

$$R^* = R^*_{L_1=0}+[L_1/b][b^2/a^2-1] \quad , \quad x=a/b$$

$$R^* = R^*_{L_1=0}+[L_1/b][1/x^2-1]$$

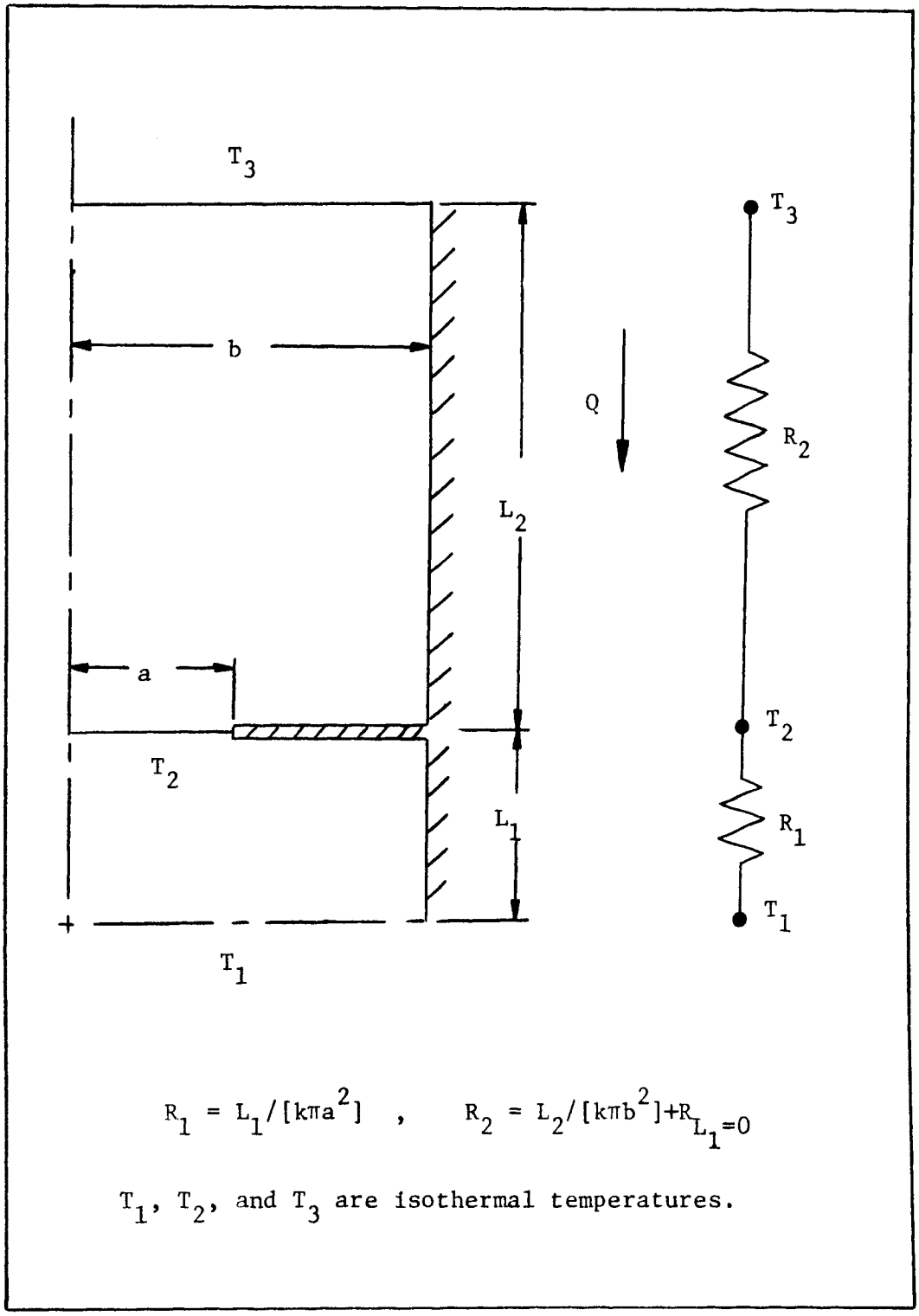

$$R_1 = L_1/[k\pi a^2] \quad , \quad R_2 = L_2/[k\pi b^2] + R_{L_1=0}$$

T_1, T_2, and T_3 are isothermal temperatures.

Figure 9. One-Dimensional Model

APPENDIX D - Method for Reconstruction of Clausing's Data

The following equation, which uses Clausing's [6] data, generates values within one percent of the center member length model.

$$R^{*}_{L_1/b=u} = R'_{L/b=\infty} = R'_{L/b=u}$$

R' is the dimensionless contact resistance obtained from Clausing's two cylinder rod model. u corresponds to a value $0< u< 1$. The Lagrangian method of extrapolation was employed to generate $R'_{L/b=u}$ from Clausing's table. The physical model, as constructed from Clausing's data, does not exist.

APPENDIX E - Dimensionless Interface Temperature Deviation

The following is a typical data set of interface temperature deviations. T_{max} and T_{min} are the maximum and minimum temperatures at the contact surface. The data is for the constriction ratio, x=0.625. L_1/b is member length and ϕ is dimensionless interface temperature deviation. $[T_i-T_o]$ in equation (14) is 2.

L_1/b	T_{max}	T_{min}	ϕ (%)
0	1.000	1.000	0
0.083	0.800	0.730	3.5
0.167	0.631	0.566	3.25
0.250	0.499	0.488	0.55
0.500	0.254	0.252	0.1
1.000	$.16\text{x}10^{-4}$	$.14\text{x}10^{-4}$	0

Table II. Dimensionless Interface Temperature Deviation